



Isotopic apportionment of sulfate aerosols between natural and anthropogenic sources in the outflow of South Asia

Sean Clarke¹, Henry Holmstrand¹, Krishnakant Budhavant^{2,3}, Manoj Remani¹, Sophie Haslett¹, Katerina Rodiouchkina^{4,5}, Ellen Kooijman⁶, Örjan Gustafsson¹ 4

- 5
- ¹ Department of Environmental Science, Stockholm University, 11418 Stockholm, Sweden.
- ² Maldives Climate Observatory at Hanimaadhoo, H. Dh. Hanimaadhoo, The Maldives
- ³ Divecha Centre for Climate Change, Indian Institute of Science, Bangalore, Karnataka 560012, India
- ⁴ Division of Geosciences, Luleå University of Technology, 971 87 Luleå, Sweden
- 10 ⁵ ALS Scandinavia AB, 977 75, Luleå, Sweden
- 11 ⁶ Department of Geosciences, Swedish Museum of Natural History, Box 50 007, Stockholm, SE-104 05, Sweden
- 13 Corresponding authors: Orjan.Gustafsson@aces.su.se; Sean.Clarke@aces.su.se

14

12

1

https://doi.org/10.5194/egusphere-2025-5334 Preprint. Discussion started: 1 December 2025 © Author(s) 2025. CC BY 4.0 License.





Abstract

Sulfate aerosols cool the climate and thus temporarily mask climate warming, but at a cost to air quality. Their short atmospheric lifetime leads to heterogeneous global coverage, with sulfate concentrations over South Asia being especially elevated and continuing to increase. It remains challenging to constrain the relative importance of different emission sources due to poor observational coverage and uncertainties in bottom-up technology-based emission estimates. The stable sulfur isotope composition ($\delta^{34}\text{S-SO4}^2$) quantitatively distinguishes natural and anthropogenic sources. This study aimed to constrain the sources of sulfate arriving at the Maldives Climate Observatory Hanimaadhoo (MCOH), which is ideally situated for intercepting the outflow from airsheds over the Indian subcontinent. The results show that anthropogenic sources of sulfate contributed 94 ± 11 %, 88 ± 9 %, and 67 ± 13 % in winter (post-monsoon), spring (pre-monsoon), and summer (monsoon), respectively. There was also a moderate to strong correlation ($r^2 = 0.79$, p << 0.05, n = 7) between continental anthropogenic (winter and spring) sulfate ($\delta^{34}\text{S}$) and black carbon aerosols from fossil fuel combustion (pinpointed by $\Delta^{14}\text{C}$). This study provides improved constraints on sulfate sources for South Asia – a key region for aerosol pollution and aerosol masking of climate warming.





1 Introduction

33 34 Anthropogenic aerosols cause substantial net negative climate forcing, which is currently attenuating the warming 35 caused by the emissions of greenhouse gases. Sulfate aerosols represent the largest component of this aerosol-36 induced masking of climate warming and the health-affecting deterioration of air quality. Sulfate aerosols are 37 primarily secondary aerosols formed from the oxidation (via H₂O₂, O₃, OH, transition metals, NO₂) of sulfur 38 dioxide, hydrogen sulfide, and sulfur-bearing organic substances, emitted from numerous natural and 39 anthropogenic sources (e.g., Berresheim et al., 2002; Szopa et al., 2021). These aerosols then alter the climate 40 through the direct (scattering of light) and indirect effects (primarily alteration of cloud properties), leading to a 41 net cooling effect (e.g., Charlson et al., 1991; Szopa et al., 2021). 42 These climatic effects are associated with the ubiquitous presence of sulfate aerosols in the atmosphere, leading 43 to an effective radiative forcing (ERF) of -0.94 Wm⁻² [-1.63 to -0.25 Wm⁻²] (Szopa et al., 2021). However, the 44 aerosols' short atmospheric lifetime (1-2 weeks) is expected to lead to a rapid readjustment once emissions change. 45 There have been regional reductions in sulfate emissions in North America and Europe for several decades. While 46 these reductions are significant environmental legislative successes, emission patterns shifted eastwards towards 47 Asia. The rise in emissions in East Asia led to a brief increase in global emissions at the start of the 21st century 48 (McDuffie et al., 2020). However, subsequent successful mitigation efforts primarily in China have dramatically 49 decreased sulfate loadings in the recent decade (McDuffie et al., 2020). The emissions from India surpassed those 50 of China at the end of the last decade (Li et al., 2017); South Asia is currently the epicenter of sulfate emissions, 51 with emissions still believed to be on the rise (McDuffie et al., 2020). 52 South Asia experienced rapid industrialization and economic growth in the latter part of the 20th century that have 53 continued into the present day, with the unintended consequence of high aerosol emissions. These loadings are 54 shown by the increasing trend over the last few decades in the aerosol optical depth (AOD), with sulfate being a 55

large contributor to this increase (Aas et al., 2019; Gupta et al., 2023). These high aerosol loadings must be addressed as they are a major health and environmental burden on South Asia, which is home to almost a quarter of the world's population (Lelieveld et al., 2020). However, our knowledge about sulfate sources and emissions remains uncertain with notable disparities between estimates from emission inventories and from remote sensing (Elguindi et al., 2020; Sharma and Kumar, 2016). The understanding of sulfate emissions is further hampered by uncertainties in natural emissions, such as oceanic dimethyl sulfide (DMS), which has seasonal and regional emission fluctuations ranging by a factor of 10-100 (Norman et al., 1999, 2004; Shenoy and Kumar, 2007). These uncertainties lead to large variations in estimates of natural versus anthropogenic contributions, especially in locations surrounded by oceans such as South Asia (Norman et al., 1999, 2004; Shenoy and Kumar, 2007). Quantitative top-down source-diagnostic isotopic composition, in combination with consideration of air-mass origins, presents an opportunity to quantitatively apportion the relative contributions from anthropogenic and natural sources of sulfate for the wider receptor atmosphere of South Asia.

67 68

69

56

57

58

59

60

61

62

63

64

65

66

Isotopic composition allows for the quantitative separation of natural versus anthropogenic sources of sulfate through distinct source end-member compositions (source fingerprints). The use of δ^{34} S for separating natural vs





- 70 anthropogenic sources is established, with a few pioneering studies now also in South Asia (Dasari and Widory,
- 71 2024; Rastogi et al., 2020; Sawlani et al., 2019).
- 72 This study employs isotopic δ³⁴S source apportionment of SO₄²⁻ to quantify the anthropogenic sulfate
- 73 contributions to the expansive airshed outflow from South Asia (representative of the wider system of the regional
- 74 aerosol-climate effect). The present study has a much wider footprint and longer time coverage than earlier studies
- 75 in the region. Distinguishing the relative source contributions of the climate-affecting sulfate in the South Asia
- 76 region provides guidance for future mitigation strategies and also provides observation-based constraints useful
- 77 for climate models.

80

2. Methods

2.1 Site description and meteorological context

- 81 South Asia encompasses several climate zones with its climate being primarily driven by the South Asian
- 82 monsoon. The monsoon season marks the onset of frequent precipitation events and the reversal of the prevailing
- 83 northerly winds. The southerly monsoon winds transport air masses from the Indian Ocean to the continent.
- 84 Seasonal oscillation also occurs in the zonal (east-west) wind component, with stronger easterlies during winter
- 85 and autumn (from the Bay of Bengal), and more westerly flow in spring (from the Arabian Sea).
- 86 Meteorologically, this leads to air masses from the high-emission region of the Indo-Gangetic Plain (IGP) being
- 87 transported into the Bay of Bengal in winter/autumn with dispersal of their anthropogenic load also over the
- 88 northern Indian Ocean (see Fig. 1). The IGP is a fertile, densely populated and highly industrialized region
- 89 spanning several countries. The IGP contributes the highest aerosol loading in South Asia and strongly impacts
- 90 aerosol loadings far out over the Indian Ocean (Aswini et al., 2020; Budhavant et al., 2024; Nair et al., 2023;
- 91 Ramanathan et al., 2001; Verma et al., 2012).
- The Maldives Climate Observatory at Hanimaadhoo (MCOH; 6°46′34″N, 73°10′59″E; tower inlet at 15 m agl) is
- 93 ideally situated for intercepting air masses arriving from the polluted and polluting IGP, the subcontinent at large,
- 94 and additionally from the open Indian Ocean during the summer (see Fig. 1). As the IGP is the key source region
- 95 of anthropogenic aerosols, two additional sites were chosen in this emission region to constrain its anthropogenic
- 96 sulfate signature. These sites were the Delhi branch of the Indian Institute of Tropical Meteorology (IITM-Delhi;
- 97 28°35′N, 77°12′E; 15 m agl) and the Bangladesh Climate Observatory Bhola (BCOB; 22°17′00″N, 90°42′36″E,
- 98 10 m agl) (see Fig. 1). Detailed information on the observatory sites can be found in previous studies (e.g., Bikkina
- 99 et al., 2019; Dasari et al., 2019).

2.2 Collection of aerosols

- 101 Samples for stable sulfur isotope measurements of sulfate in this study were hence collected from three sites in
- 102 South Asia. The urban PM_{2.5} filters (47 mm diameter quartz filters, Millipore) were collected from the IITM-Delhi
- in the winter of 2016 (January and February) using a high-volume sampler (APM 550 Envirotech, flow rate = 1
- 104 m³ hr⁻¹, time = 12 hours). The IGP outflow PM_{2.5} filters were collected at BCOB in the winter of 2016 (January),
- using a high-volume sampler (model DH77, DIGITEL A.G., Switzerland, flow rate = 500 L min⁻¹, time = 24
- 106 hours). The integrating filters of the South Asian outflow, intercepted over the Indian Ocean, were collected at
- 107 MCOH with sample dates spanning several years (winter = 2016, summer = 2013-2015, spring = 2013) (winter =





- 108 PM₁, spring and summer = PM_{2.5}) using a high-volume sampler (model DH77, DIGITEL A.G., Switzerland, flow
- 109 rate = 500 L min⁻¹, time = 24 hours). Detailed information on the collection of aerosol samples can be found in
- previous studies (e.g., Kirillova et al., 2013, 2014).

111 **2.3 Ionic concentrations**

- 112 Ionic concentrations (Cl⁻, Br⁻, NO₂⁻, NO₃⁻, PO₃⁴, SO₄², Na⁺, NH₄⁺, K⁺, Mg²⁺, Ca²⁺) were measured using a
- 113 Dionex Aquion ion chromatography (IC) system (Thermo Finnigan LLC). Cut-outs (1-4 cm²) of the filter samples
- 114 were dissolved in 10 mL of Milli-Q water and analyzed with a flow rate of 1 mL min⁻¹. Standards and field blanks
- were used to ensure quality control and minimize external influences.
- The sea spray fraction of SO₄² was removed following (Keene et al., 1986), as shown in Eq. (1):

117
$$nssSO_4^{2-} = [SO_4^{2-}] - [(\frac{[SO_4^{2-}]}{[Na^+]})_{sea} \times [Na^+]$$
 (1)

- The nss-SO₄²⁻ is the non-sea salt sulfate, with the ratio of sulfate to sodium from sea water being 0.253 taken
- 119 from (Keene et al., 1986). Seawater is enriched in sulfate due to long-term accumulation. This results in natural
- 120 emissions of sulfate aerosols from sea spray, which must be accounted for to enable accurate source apportionment
- 121 of nss-SO₄²-.

122

123 2.4 Isotopic analysis

124 **2.4.1** Analysis of δ^{34} S

- The determination of the $\delta^{34}S$ composition of aerosols on 17 carefully selected samples was performed following
- 126 the method described in detail in Rodiouchkina, 2018. Filter cut-outs were placed in polypropylene tubes and
- 127 Milli-Q water was added to extract the sulfate (5 h in an ultrasonic bath). Sulfur was then isolated using anion
- exchange chromatography (AG 1-X8, analytical grade, 200-400 mesh, chloride form, Bio-Rad Laboratories,
- 129 USA). The standards (S1, S3, and S4 from IAEA, Austria) and samples were then diluted to an S concentration
- 130 of 2 µg mL⁻¹ before being run in a solution matrix of 0.3 M HNO₃ (sub-boiled). Silicon (Si) was added to all
- 131 solutions at a concentration ratio of 1:1 (S:Si, µg mL⁻¹:µg mL⁻¹) for internal standardization. Additionally, sodium
- 132 (Na) was added at a molar ratio of 2 (Na/S) to all measurement solutions. The measurements were carried out
- 133 using a multi-collector inductively coupled plasma mass spectrometer (MC-ICP-MS, Nu Plasma II, Nu
- 134 Instruments, UK) and run-in dry plasma mode using a desolvator (Aridus II, CETAC, USA) at the Vegacenter
- 135 facility of the Swedish Museum of Natural History, Stockholm, Sweden. Detailed descriptions and typical
- 136 operating parameters can be found in Rodiouchkina, 2018. For instrument settings and parameters see Method
- 137 S1.

138 139

2.4.2 Analysis of radiocarbon (Δ¹⁴C) composition in Black Carbon (BC)

- 140 A total of 14 samples for Δ^{14} C were prepared for dual isotopic analysis of combustion-derived BC (MCOH spring
- 141 = 2, MCOH summer = 3, BCOB = 3, MCOH winter = 6). The winter samples comprise data taken from Dasari et
- 142 al., 2020. Inorganic carbonates were removed by acid fumigation (12 M HCl) for 24 h, then the samples were
- dried at 60 °C for 1 h. The samples were subjected to thermal-oxidation separation of OC from BC using a TOT
- analyzer (Thermal Optical Transmittance, Sunset Laboratory, Tigard, Oregon, USA) and the resulting carbon





- dioxide derived from the BC fraction was trapped using a custom-built system described and extensively tested
- earlier (e.g., Andersson et al., 2015; Chen et al., 2013; Winiger et al., 2015). The trapped CO₂ from the BC fraction
- 147 was then sent to the collaborating Accelerator Mass Spectrometry facility (AMS) at Uppsala University (Sweden)
- 148 for Δ^{14} C isotopic analysis. The source apportionment was calculated using Eq. (2) and Eq. (3), with end-member
- values taken from the literature (Andersson et al., 2015; Bikkina et al., 2019).

150
$$\Delta^{14}C_{BC} = \left[F_m \times e^{\frac{-(x_{year}-1954)}{8267}} - 1\right] \times 1000$$
 (2)

152
$$\Delta^{14}C_{BC} = \Delta^{14}C_{biomass} \times F_{bio-BC} + \Delta^{14}C_{fossil} \times (1 - F_{bio-BC})$$
 (3)

153 154

- 2.5 Model for apportioning between natural and anthropogenic sulfur input
- 155 The approach to apportion natural versus anthropogenic sulfate was carried out in several steps. First, the data
- 156 were corrected for the minor contribution from sea spray based on the well-known isotopic composition of sea
- 157 water using Eq. (4). The sample MCOH PM₁_13-14/01/2016 was corrected using the fraction of non-sea salt
- 158 contribution to tot-SO₄ from the other samples (98.9 \pm 0.2 %) due to sample depletion.

159
$$\delta^{34}S_{nss} = \left(\delta^{34}S - \left(\frac{100 - \%nssSO_4}{100}\right) \times \delta^{34}S_{sea\ water}\right) \div \frac{\%nssSO_4}{100}$$
 (4)

- 160 The isotopic composition of $\delta^{34}S_{sea water}$ is $+21 \pm 0.2$ % from Böttcher et al., 2007 and Rees et al., 1978. The
- percentage of nss-SO₄²⁻ is determined from Eq. (1).
- 162 After this correction, the nss- δ^{34} S was used in a binary model to apportion the relative contributions from
- anthropogenic-fossil sources (e.g., ship emissions/IGP sources) vs the marine biogenic (DMS) source, using Eq.
- 164 (5):

165

$$\delta^{34}S_{nss} = \delta^{34}S_{DMS} \times F_{DMS-SO4} + \delta^{34}S_{anthropogenic} \times (1 - F_{DMS-SO4})$$
(5)

167

- where F represents the fraction (DMS and anthropogenic), $\delta^{34}S_{nss}$ represents the $\delta^{34}S$ of the sample, $\delta^{34}S_{DMS}$
- and $\delta^{34}S_{anthropogenic}$ refer to the mean isotopic composition of the end-members (DMS and anthropogenic). The
- 170 DMS end-member was taken from Amrani et al., 2013, with a δ^{34} S composition of +19.7 \pm 0.5 \(\text{\text{\text{\text{M}}}}.\) The
- anthropogenic end-member varies by season and is constrained by a combination of literature reports and new
- findings in this study. For samples where air masses originated from the continent (spring, winter), an IGP end-
- member was used. The IGP end-member had a δ^{34} S of 2.3 \pm 1.7 ‰ calculated from this study and literature (Dasari
- and Widory, 2024; Sawlani et al., 2019, Table S1). The ship end-member had a δ^{34} S of 3 ± 3 % taken from studies
- that measured δ^{34} -SO₄ and δ^{34} -SO₂ in the North Atlantic, which is thought to be representative of remote air
- masses with strong ship emissions from heavy fuel oil.





179 2.6 Satellite imagery and computational analysis The Hybrid Single-Particle Lagrangian Integrated Trajectory (HYSPLIT) model was used to run 7-day backward 180 181 trajectories from the NOAA Air Research Laboratory (available at http://ready.arl.noaa.gov/HYSPLIT.php). Back 182 trajectories for seasonal clusters were calculated for summer (June-September 2015), winter (December-March 183 2015-2016) and spring (April-May 2015). 184 MERRA-2 (Modern-Era Retrospective Analysis for Research and Applications, version 2) and TROPESS 185 (TRopospheric Ozone and its Precursors from Earth System Sounding) were used to retrieve model-estimated 186 surface concentrations of black carbon and sulfate. MERRA-2 is a reanalysis product that uses remote sensing 187 aerosol optical depth (satellite- and ground-based) in combination with the Goddard Earth Observing System 188 Model, Version 5 to calculate aerosol concentrations (Buchard et al., 2017; Gelaro et al., 2017; Randles et al., 189 2017). TROPESS includes additional satellite measurements (TES, AIRS, TROPOMI, and OMPS) combined 190 with a retrieval algorithm to obtain sulfate surface concentrations (Miyazaki, 2024). 191 192 2.7 Emission inventory 193 The Community Emissions Data System (CEDSv2021_04_21) is a bottom-up emission inventory that provides 194 gridded and national fluxes of short-lived climate pollutants (Hoesly et al., 2018). The national inventory dataset 195 is available at https://zenodo.org/records/4741285.

3 Results and discussion





197 198	3.1 Constraints on isotopic signatures of different sources Reports on the isotopic composition of sulfate from different sources and regions display a large range, although
199	marine natural sources are clearly enriched in ³⁴ S compared to anthropogenic sources. Natural sources
200	considered in this study were sea spray and dimethyl sulfide (DMS), the dominant marine biogenic source. Sea
201	spray and DMS have a well-defined isotopic composition of $+21 \pm 0.2$ % and $+19.7 \pm 0.5$ %, respectively
202	(Amrani et al., 2013; Böttcher et al., 2007; Rees et al., 1978). In contrast, fossil fuel end-members can vary (-35
203	to +33 %) depending on fuel type (liquid vs solid), as well as having strong geographical differences
204	(Jongebloed et al., 2023; Lee et al., 2023). Additional details on sulfate sources and considerations in sulfur-
205	isotopic attribution studies are provided in the Supplementary Information (Text S1).
206	To account for the potential variability in fossil fuel isotope end-members, an anthropogenic end-member was
207	determined through sampling in the regional source-integrating air masses of the IGP, with end-member
208	uncertainty accounted for through error propagation (see Method S2). The samples were first split based on air
209	mass origin into a continental anthropogenic end-member and an oceanic anthropogenic end-member. The
210	oceanic anthropogenic input was expected to be predominantly from ship emissions, with a $\delta^{34}S$ signature of 3 \pm
211	3 ‰ taken from the literature on the marine anthropogenic end-member (Seguin et al., 2010, 2011; Wadleigh,
212	2004, Text S1).
213	The integrated continental anthropogenic signature was calculated from the IGP samples in this study and from
214	the literature, resulting in an end-member value of 2.3 ± 1.7 % (see Fig. 2, Table S1; Dasari & Widory, 2024;
215	$Sawlani\ et\ al.,\ 2019,\ n=50).\ Anthropogenic\ sulfate\ also\ includes\ minor\ contributions\ from\ crustal\ and\ biomass$
216	burning sources, which have not been separated in this study (Dasari and Widory, 2024). The average from this
217	study was slightly lower due to one sample showing a near-zero $\delta^{34}S$ value (-0.07 ‰). This $\delta^{34}S$ -depleted
218	sample likely reflects sulfate formation through oxidation catalyzed by transition metal ions (TMI) and is
219	associated with poor air quality, reported during hazy conditions (Harris et al., 2013; Sawlani et al., 2019).
220	Alternatively, this type of isotope depletion has been proposed to be related to increased coal input or
221	terrigenous sulfate (Dasari and Widory, 2024). These depleted oxidative pathways/sources are likely to occur as
222	a continuum, motivating the inclusion of the depleted sample.
223	
224 225	3.2 Abundance of sulfate aerosols over the northern Indian Ocean There are only limited reports of measured sulfate concentrations over the Indian Ocean, an area integral to South
226	Asia's monsoon/hydrological cycles and aerosol-affected regional climate forcing. This reduces the confidence in
227	our understanding of the regional loadings of sulfate and the effective regional climate forcing. The loadings for
228	the non-sea salt sulfate (nss-SO ₄ ²⁻) over the northern Indian Ocean for winter, spring, and summer in this study
229	were $10 \pm 4 \ \mu g \ m^{-3} \ (96 \pm 6 \ \% \ nss-SO_4{}^2$, full period $n = 43 \ from \ Dasari et al., 2019), 5.5 \pm 1 \ \mu g \ m^{-3} \ (98.5 \pm 0.1 \ \% \ nss-SO_4{}^2$
230	nss-SO ₄ ²⁻), $1 \pm 0.2 \mu g m^{-3}$ (85.5 \pm 5.5 % nss-SO ₄ ²⁻), respectively, with these values broadly agreeing with previous properties of the second sec
231	reports from the MCOH receptor of the South Asian outflow (Budhavant et al., 2023, 2024b).
232	Seasonal differences are due to both fluctuating emissions and varying seasonal air transport from the source
233	regions (Fig. 1). These meteorological factors (wind speed, boundary layer height, humidity, etc.) cause winter
234	conditions to be favorable for long-range aerosol transport from the polluted IGP out over the northern Indian





235 Ocean (Aswini et al., 2020; Dasari et al., 2019; Kesti et al., 2020; Ram et al., 2012). With a shortage of in situ measurements, estimates from remote sensing provide a picture of sulfate loadings for remote regions; expansion 236 237 of in situ atmospheric observatory measurements is critical to the validation of the accuracy of derived estimates 238 from remote sensing. 239 Remote sensing estimations of sulfate loadings are commonly derived from optical measurements of columnar 240 data, which can differ greatly from ground conditions. The indirect estimates of sulfate surface loadings from 241 remote sensing (MERRA-2, TROPESS at p= 1000 hPa) were 2-5 times lower than the in situ sulfate measurements 242 in this study (see Fig. S1). These discrepancies need to be confirmed by forthcoming longer and more complete 243 in situ measurement records of sulfate in this critical region for sulfate-climate effects. Long-term in situ records 244 remain pivotal in understanding long-term changes, which become even more valuable when combined with 245 additional analysis such as isotopic source apportionment. 246 247 3.3 Source-diagnostic isotopic composition of sulfate aerosols over the northern Indian Ocean 248 Refined constraints on sulfate sources improve our understanding of the atmospheric cycle of climate-forcing 249 anthropogenic sulfate over South Asia. The study results show that anthropogenic sulfate dominated in the South 250 Asian outflow intercepted over the northern Indian Ocean, yet there is also substantial input of natural sulfate, 251 especially in the monsoon period. The input of anthropogenic sources to the nss- SO_4^{2-} loading was $94 \pm 11 \%$, 88 252 \pm 9 %, 67 \pm 13 % for winter, spring (pre-monsoon), and summer (monsoon), respectively (Fig. 2; Table S1). 253 These fractions translate into anthropogenic sulfate concentrations of $0.6 \pm 0.2 \,\mu g \, m^{-3}$ (summer), $4.6 \pm 0.7 \,\mu g \, m^{-3}$ 254 3 (spring) and $9.1 \pm 5 \,\mu g \, m^{-3}$ (samples with $\delta 34S$; winter). Although the summer conditions are cleanest, the region 255 is still highly affected by anthropogenic input, with freight ships during that time likely being an important source. 256 Three major shipping lanes cross the northern Indian Ocean. During the study period, the global shipping 257 emissions were nearly equal to the cumulative emissions of South Asia (McDuffie et al., 2020). These loadings 258 are elevated given the remote location, even with respect to health guidelines for exposure to fine particulate 259 matter. 260 The World Health Organization (WHO) annual guideline for PM_{2.5} is 5 µg m⁻³ (World Health Organization, 2021), 261 a limit which is frequently exceeded in both winter and spring even this far out over the Indian Ocean, despite 262 local emissions being documented to be low (Budhavant et al., 2015). It is worth noting that a portion of the sulfate 263 loading in the winter air masses from the Bay of Bengal may possibly be influenced by input from mangroves, 264 which emit hydrogen sulfide (H_2S). This gas is rapidly oxidized and typically has a $\delta^{34}S$ below 0 ‰ (Jamieson & 265 Wadleigh, 1999). The H₂S flux from mangroves is potentially significant with emissions estimates ranging from 266 approximately 10 - 25 % of South Asia's anthropogenic emissions (Ganguly et al., 2018; Hoesly et al., 2018). 267 However, analysis of the back trajectories suggests that sulfate loadings were influenced more by seasonal 268 variation than by specific trajectory pathways (see Fig. S2). Sulfate loadings reaching MCOH are elevated and 269 are attributed primarily to anthropogenic sources. 270 This isotope-based source apportionment of sulfate in the receptor-integrated South Asian outflow appears

broadly consistent with other regional studies. A study over the northern Bay of Bengal reported $\delta^{34}S = 4.5 \pm$

1.3‰ in PM10 during February-April 2013 (Rastogi et al., 2020). Applying our δ34S two-end-member mixing

271





model to those Port Blair PM₁₀ values indicates that at least ~90% of sulfate was anthropogenic. This should be viewed as a conservative lower bound because the sea-salt contribution for the isotopic data was not reported (so no sea-salt correction could be applied), and PM₁₀ generally contains a larger sea-salt fraction. Similarly, the ICARB-2018 ship campaign estimated anthropogenic sulfate to make up 96 % of the nss-SO₄²⁻ in the Arabian Sea and Indian Ocean (Aswini et al., 2020), using the ratio of methanesulfonic acid (MSA)/nss-SO₄²⁻. These results suggest a quite limited influence of DMS on the total sulfate mass balance over the northern Indian Ocean, even though globally DMS emissions are expected to be a quarter the size of anthropogenic emissions (Lana et al., 2011). These results provide quantitative constraints on sources, showing a strong dominance of anthropogenic sources of sulfate in the northern Indian Ocean, yet with seasonal variations.

3.4 Relationships between sulfate and black carbon

Sulfate precursors and black carbon (BC) are both emitted in large quantities from fossil fuel combustion, yet they also have other separate sources. We explored the extent of co-emission of these two short-lived climate pollutants (SLCPs), having opposing signs in their climate forcing. By comparing isotope-based source indicators (δ^{34} S–SO₄ and Δ^{14} C–BC), we observe a positive correlation ($r^2 = 0.79$, p << 0.05, n = 7) between anthropogenic sulfate and the fraction of BC attributed to fossil fuel combustion for the outflow receptor observatory at MCOH (winter and spring) (see Fig. 3 inset). Samples from BCOB, which were used to represent the anthropogenic end-member of sulfate, were assumed to be predominantly anthropogenic in origin (~100 %), although minor contributions from dust and biomass are expected (Dasari and Widory, 2024). Summer data were too limited for robust conclusions, although a similar pattern was observed, potentially reflecting differences in emission sources (see Fig. S3). The positive correlation between the isotope fingerprints of these SLCPs lends further credence to the δ^{34} S-based findings that fossil fuel combustion is indeed a major source of SO₄²⁻ over South Asia, with additional insight provided by examining the relationship between SO₄²⁻ and climate-warming BC.

Black carbon and sulfate, in part co-emitted, have opposite climatic effects, with BC enhancing climate warming while sulfate masks climate warming. Their opposing climatic effects lead to large uncertainties in radiative forcing due to the ratio of scattering vs absorbing vectors, especially in regions with high loadings of both BC and SO_4^{2-} , such as South Asia (Li et al., 2022). The BC/ SO_4^{2-} ratio for the study period was 0.075 ± 0.03 (spring and winter; summer was excluded due to high variability). The BC/SO₄²⁻ ratio in the surface layer estimated from remote sensing by MERRA-2 was much higher for winter during which it was predicted to be 0.16 (2016) and for spring (April 2013) during which it was predicted to be 0.15; both were twice overestimated compared to our direct in situ measurements. The observed BC/SO₄²⁻ ratio was compared with an inventory-based BC/SO₂ ratio from the Community Emissions Data System (CEDS v2021-04-21). The BC/SO2 ratio was obtained by aggregating BC and SO₂ fluxes over India, Pakistan, and Bangladesh. As inventories report SO₂ (not sulfate), BC/SO₂ is used as a proxy for BC/SO₂²⁻. The ratio from CEDS was 0.097 (2015-2019 average; Hoesly et al., 2018), which is close to the BC/SO_4^{2-} ratio of 0.075 ± 0.03 constrained by in situ measurements in the current study, with MERRA-2 being higher. There is a need for increased comparison of BC/SO₄²⁻ (and their sources) simulated by models and predicted by emission inventories with greater datasets of in situ observations in South Asia, given the expected changes in their respective emissions and that reduced SO₄²- emissions will unmask current climate warming for the region.





313 4 Conclusion and outlook 314 There are very large sulfate loadings over South Asia compared with the global average. However, there is poor 315 spatial coverage of actual measurements of both SO₄²⁻ and its source-diagnostic isotopic composition. This study 316 provides the first multi-seasonal isotope-based source apportionment of sulfate for the integrated outflow airshed 317 of South Asia. The quantitative results show that anthropogenic nss-sulfate is the major contributor to sulfate 318 loadings in this region, yet with clear seasonal and spatial variations and with some contributions also from 319 natural-biogenic sources (e.g., from marine plankton and possibly from mangroves). Quantitative isotope-based 320 observational constraints on the relative contributions of different sources to atmospheric sulfate are vital for both 321 understanding total emissions of this important climate forcer and for guiding strategies to mitigate the 322 anthropogenic components. 323 Future investigations should aim to constrain the long-term trend (decades) of wintertime and summer sources of 324 sulfate to the South Asian airshed. This will improve the understanding of emission patterns from the heavily 325 polluted IGP, as well as provide potential insights into atmospheric processing due to South Asia's changing 326 meteorology. Aerosol loadings have already been shown to strongly affect the monsoon period (Krishnan et al., 327 2016; Ramarao et al., 2023). Moreover, both current and past emissions will be needed to understand future 328 changes, with emissions expected to decrease due to socio-economic pressures. Thus, there is an urgent need for 329 improved understanding of all facets of sulfate aerosols to help improve resilience against future climatic impacts, 330 including the extent to which we may need to anticipate enhanced warming (with South Asia being particularly 331 sensitive to heat extremes) due to the demasking of climate warming caused by decreasing sulfate loadings. 332 Additional information 333 Additional information can be found in the attached Supplementary Information. Data are available in the Bolin 334 Centre Database (DOI: 10.17043/clarke-2025-v3m0nk-1). 335 336 Author contributions 337 This study was conceptualized by Ö.G. and H.H. Atmospheric sampling strategies and campaign execution were 338 realized by K.B., H.H. and Ö.G. Laboratory procedures, data quality assessments and calculations were 339 performed by M.R., S.C., H.H., K.R. and E.K. Interpretations and the first draft of the manuscript were 340 primarily contributed by H.H., Ö.G., S.C. Finally, S.C. produced all display items and wrote the manuscript 341 with all authors contributing to detailed data interpretation and writing. 342 343 Acknowledgements 344 Elena Kirillova and Srinivas Bikkina (Stockholm University) are acknowledged for their support during the 345 field campaigns. We thank the technical staff at the BCOB and MCOH for their continued field support. Special 346 thanks are due to the Maldives Meteorological Service and the government of the Republic of Maldives for their

ongoing support of the joint MCOH operation. Krishnakant Budhavant expresses thanks for the additional

Technology (AIT), Thailand. This is Vegacenter publication number [to be assigned after the paper accepted].

support from the Regional Resource Centre for Asia and the Pacific (RRC.AP) at the Asian Institute of

347

348

https://doi.org/10.5194/egusphere-2025-5334 Preprint. Discussion started: 1 December 2025 © Author(s) 2025. CC BY 4.0 License.



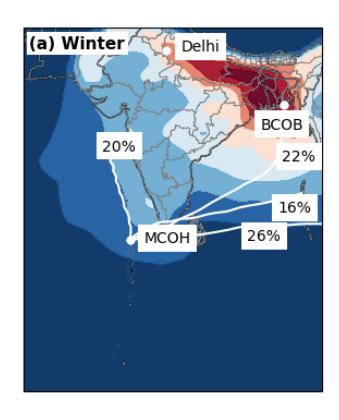


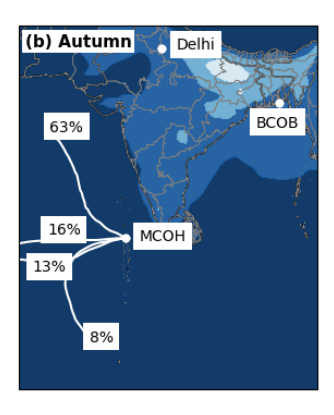
350	
351 352	The authors acknowledge the use of the ChatGPT large-language model (OpenAI) for grammar and language editing assistance; all scientific content and interpretations are the authors' own.
353	
354	Financial support
355	This research was funded by the Swedish Research Council (VR Grant 2017-01601 to ÖG), the Swedish
356	$Research\ Council\ for\ Sustainable\ Development\ (FORMAS\ Grant\ 2023-01234\ to\ \ddot{O}.G.).\ We\ also\ acknowledge$
357	the Swedish Research Council (VR) for financial support to the NordSIMS-Vegacenter national research
358	infrastructure (Grant 2017-00671).
359	
360	Competing interests
361	The authors declare that they have no conflict of interest.
362	

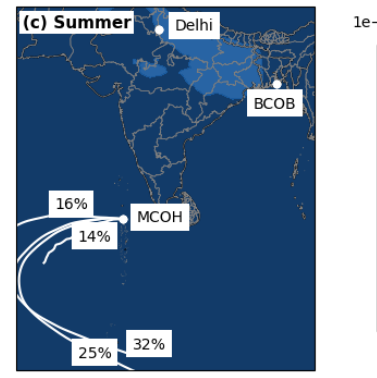




363 364 **Figures** 365







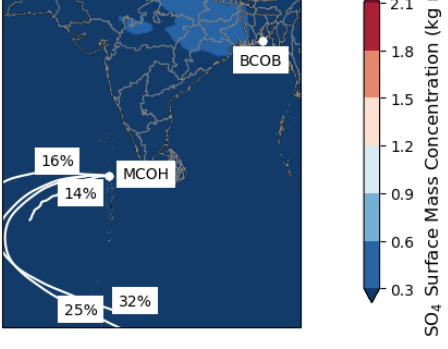


Fig. 1. Remote sensing estimates of sulfate surface concentration (MERRA-2) and average back trajectories (7-day clusters; HYSPLIT, white lines depict the mean paths of the HYSPLIT back-trajectory clusters) for South Asia, for three seasons: (a) winter (December–March 2015– 2016); (b) spring (April–May 2013); (c) summer (June–September 2015).





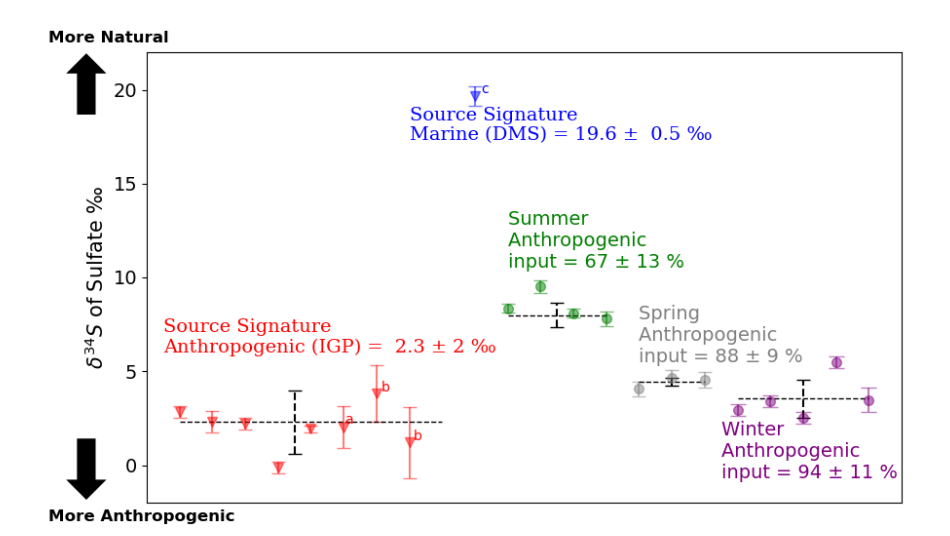


Fig. 2. Sulfate δ^{34} S composition for MCOH and end-members: IGP source signature (this study, n = 5; a = Dasari & Widory, 2024, n = 15; b = Sawlani et al., 2019, n = 30), DMS source signature (blue; c = Amrani et al., 2013, n = 16). MCOH summer (green), spring (grey), and winter (purple). Error bars for this study's samples show $\pm 4\sigma$ (instrumental analytical precision, per measurement). Literature points and seasonal aggregates show $\pm 2\sigma$ (between-sample standard deviation).





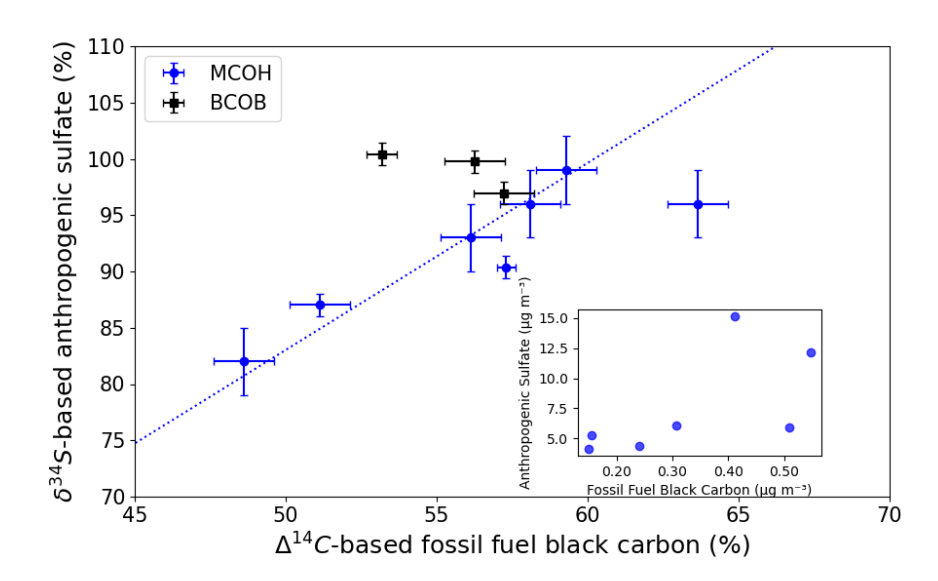


Fig. 3. Relationships between fossil fuel black carbon and anthropogenic sulfate for MCOH (spring, summer; blue circles) and BCOB (black squares), calculated using isotopic composition (Δ^{14} C, δ^{34} S). The inset graph shows the actual concentrations of fossil fuel black carbon and anthropogenic sulfate for MCOH.





383

384

References

- Aas, W., Mortier, A., Bowersox, V., Cherian, R., Faluvegi, G., Fagerli, H., Hand, J., Klimont, Z.,
- 386 Galy-Lacaux, C., Lehmann, C. M. B., Myhre, C. L., Myhre, G., Olivié, D., Sato, K., Quaas, J., Rao, P.
- 387 S. P., Schulz, M., Shindell, D., Skeie, R. B., Stein, A., Takemura, T., Tsyro, S., Vet, R., and Xu, X.:
- 388 Global and regional trends of atmospheric sulfur, Sci Rep, 9, https://doi.org/10.1038/s41598-018-
- 389 37304-0, 2019.
- 390 Amrani, A., Said-Ahmad, W., Shaked, Y., and Kiene, R. P.: Sulfur isotope homogeneity of oceanic
- 391 DMSP and DMS, Proc Natl Acad Sci U S A, 110, https://doi.org/10.1073/pnas.1312956110, 2013.
- 392 Andersson, A., Deng, J., Du, K., Zheng, M., Yan, C., Sköld, M., and Gustafsson, Ö.: Regionally-
- 393 varying combustion sources of the January 2013 severe haze events over eastern China, Environ Sci
- 394 Technol, 49, https://doi.org/10.1021/es503855e, 2015.
- 395 Aswini, A. R., Hegde, P., Aryasree, S., Girach, I. A., and Nair, P. R.: Continental outflow of
- 396 anthropogenic aerosols over Arabian Sea and Indian Ocean during wintertime: ICARB-2018
- 397 campaign, Science of the Total Environment, 712, https://doi.org/10.1016/j.scitotenv.2019.135214,
- 398 2020.
- 399 Berresheim, H., Elste, T., Tremmel, H. G., Allen, A. G., Hansson, H. C., Rosman, K., Dal Maso, M.,
- 400 Mäkelä, J. M., Kulmala, M., and O'Dowd, C. D.: Gas-aerosol relationships of H2SO4, MSA, and OH:
- 401 Observations in the coastal marine boundary layer at Mace Head, Ireland, Journal of Geophysical
- 402 Research Atmospheres, 107, https://doi.org/10.1029/2000JD000229, 2002.
- 403 Bikkina, S., Andersson, A., Kirillova, E. N., Holmstrand, H., Tiwari, S., Srivastava, A. K., Bisht, D.
- 404 S., and Gustafsson, Ö.: Air quality in megacity Delhi affected by countryside biomass burning, Nat
- 405 Sustain, 2, https://doi.org/10.1038/s41893-019-0219-0, 2019.
- 406 Böttcher, M. E., Brumsack, H. J., and Dürselen, C. D.: The isotopic composition of modern seawater
- 407 sulfate: I. Coastal waters with special regard to the North Sea, Journal of Marine Systems, 67,
- 408 https://doi.org/10.1016/j.jmarsys.2006.09.006, 2007.
- 409 Buchard, V., Randles, C. A., da Silva, A. M., Darmenov, A., Colarco, P. R., Govindaraju, R., Ferrare,
- 410 R., Hair, J., Beyersdorf, A. J., Ziemba, L. D., and Yu, H.: The MERRA-2 aerosol reanalysis, 1980
- onward. Part II: Evaluation and case studies, J Clim, 30, https://doi.org/10.1175/JCLI-D-16-0613.1,
- 412 2017
- 413 Budhavant, K., Andersson, A., Bosch, C., Kruså, M., Murthaza, A., Zahid, and Gustafsson, Ö.:
- 414 Apportioned contributions of PM2.5 fine aerosol particles over the Maldives (northern Indian Ocean)
- from local sources vs long-range transport, Science of the Total Environment, 536,
- 416 https://doi.org/10.1016/j.scitotenv.2015.07.059, 2015.
- 417 Budhayant, K., Andersson, A., Holmstrand, H., Satheesh, S. K., and Gustafsson, Ö.: Black carbon
- 418 aerosols over Indian Ocean have unique source fingerprint and optical characteristics during monsoon
- 419 season, Proc Natl Acad Sci U S A, 120, https://doi.org/10.1073/pnas.2210005120, 2023.
- 420 Budhavant, K., Manoj, M. R., Nair, H. R. C. R., Gaita, S. M., Holmstrand, H., Salam, A., Muslim, A.,
- 421 Satheesh, S. K., and Gustafsson, Ö.: Changing optical properties of black carbon and brown carbon
- 422 aerosols during long-range transport from the Indo-Gangetic Plain to the equatorial Indian Ocean,
- 423 Atmos Chem Phys, 24, 11911–11925, https://doi.org/10.5194/acp-24-11911-2024, 2024.





- Charlson, R. J., Langner, J., Rodhe, H., Leovy, C. B., and Warren, S. G.: Perturbation of the Northern
- 425 Hemisphere radiative balance by backscattering from anthropogenic sulfate aerosols, Tellus, Series A-
- 426 B, 43 A-B, https://doi.org/10.3402/tellusb.v43i4.15404, 1991.
- 427 Chen, B., Andersson, A., Lee, M., Kirillova, E. N., Xiao, Q., Kruså, M., Shi, M., Hu, K., Lu, Z.,
- 428 Streets, D. G., Du, K., and Gustafsson, Ö.: Source forensics of black carbon aerosols from China,
- 429 Environ Sci Technol, 47, https://doi.org/10.1021/es401599r, 2013.
- 430 Dasari, S. and Widory, D.: Retrospective Isotopic Analysis of Summertime Urban Atmospheric
- 431 Sulfate in South Asia Using Improved Source Constraints, ACS ES&T Air, 1, 357–364,
- 432 https://doi.org/10.1021/acsestair.3c00060, 2024.
- 433 Dasari, S., Andersson, A., Bikkina, S., Holmstrand, H., Budhavant, K., Satheesh, S., Asmi, E., Kesti,
- 434 J., Backman, J., Salam, A., Bisht, D. S., Tiwari, S., Hameed, Z., and Gustafsson, Ö.: Photochemical
- 435 degradation affects the light absorption of water-soluble brown carbon in the South Asian outflow, Sci
- 436 Adv, 5, https://doi.org/10.1126/sciadv.aau8066, 2019.
- 437 Dasari, S., Andersson, A., Stohl, A., Evangeliou, N., Holmstrand, H., Budhavant, K., Salam, A., and
- 438 Gustafsson, Ö.: Source Quantification of South Asian Black Carbon Aerosols with Isotopes and
- 439 Modeling, Environ Sci Technol, 54, 11771–11779, https://doi.org/10.1021/acs.est.0c02193, 2020.
- 440 Elguindi, N., Granier, C., Stavrakou, T., Darras, S., Bauwens, M., Cao, H., Chen, C., Denier van der
- 441 Gon, H. A. C., Dubovik, O., Fu, T. M., Henze, D. K., Jiang, Z., Keita, S., Kuenen, J. J. P., Kurokawa,
- 442 J., Liousse, C., Miyazaki, K., Müller, J. F., Qu, Z., Solmon, F., and Zheng, B.: Intercomparison of
- 443 Magnitudes and Trends in Anthropogenic Surface Emissions From Bottom-Up Inventories, Top-
- 444 Down Estimates, and Emission Scenarios, Earths Future, 8, https://doi.org/10.1029/2020EF001520,
- 445 2020
- 446 Ganguly, D., Ray, R., Majumdar, N., Chowdhury, C., and Jana, T. K.: Biogenic hydrogen sulphide
- 447 emissions and non-sea sulfate aerosols over the Indian Sundarban mangrove forest, J Atmos Chem,
- 448 75, 319–333, https://doi.org/10.1007/s10874-018-9382-3, 2018.
- Gelaro, R., McCarty, W., Suárez, M. J., Todling, R., Molod, A., Takacs, L., Randles, C. A.,
- 450 Darmenov, A., Bosilovich, M. G., Reichle, R., Wargan, K., Coy, L., Cullather, R., Draper, C., Akella,
- 451 S., Buchard, V., Conaty, A., da Silva, A. M., Gu, W., Kim, G. K., Koster, R., Lucchesi, R., Merkova,
- D., Nielsen, J. E., Partyka, G., Pawson, S., Putman, W., Rienecker, M., Schubert, S. D., Sienkiewicz,
- 453 M., and Zhao, B.: The modern-era retrospective analysis for research and applications, version 2
- 454 (MERRA-2), J Clim, 30, https://doi.org/10.1175/JCLI-D-16-0758.1, 2017.
- 455 Gupta, G., Ratnam, M. V., and Madhavan, B. L.: Changing patterns in the highly contributing aerosol
- 456 types/species across the globe in the past two decades, Science of the Total Environment, 897,
- 457 https://doi.org/10.1016/j.scitotenv.2023.165389, 2023.
- 458 Harris, E., Sinha, B., Van Pinxteren, D., Tilgner, A., Fomba, K. W., Schneider, J., Roth, A., Gnauk,
- 459 T., Fahlbusch, B., Mertes, S., Lee, T., Collett, J., Foley, S., Borrmann, S., Hoppe, P., and Herrmann,
- 460 H.: Enhanced role of transition metal ion catalysis during in-cloud oxidation of SO2, Science (1979),
- 461 340, https://doi.org/10.1126/science.1230911, 2013.
- 462 Hoesly, R. M., Smith, S. J., Feng, L., Klimont, Z., Janssens-Maenhout, G., Pitkanen, T., Seibert, J. J.,
- 463 Vu, L., Andres, R. J., Bolt, R. M., Bond, T. C., Dawidowski, L., Kholod, N., Kurokawa, J. I., Li, M.,
- 464 Liu, L., Lu, Z., Moura, M. C. P., O'Rourke, P. R., and Zhang, Q.: Historical (1750-2014)
- 465 anthropogenic emissions of reactive gases and aerosols from the Community Emissions Data System
- 466 (CEDS), Geosci Model Dev, 11, 369–408, https://doi.org/10.5194/gmd-11-369-2018, 2018.





- 467 Jamieson, R. E. and Wadleigh, M. A.: A study of the oxygen isotopic composition of precipitation
- sulphate in eastern Newfoundland, Water Air Soil Pollut, 110,
- 469 https://doi.org/10.1023/a:1005002026009, 1999.
- 470 Jongebloed, U. A., Schauer, A. J., Hattori, S., Cole-Dai, J., Larrick, C. G., Salimi, S., Edouard, S. R.,
- 471 Geng, L., and Alexander, B.: Sulfur isotopes quantify the impact of anthropogenic activities on
- 472 industrial-era Arctic sulfate in a Greenland ice core, Environmental Research Letters, 18,
- 473 https://doi.org/10.1088/1748-9326/acdc3d, 2023.
- 474 Keene, W. C., Pszenny, A. A. P., Galloway, J. N., and Hawley, M. E.: Sea-salt corrections and
- 475 interpretation of constituent ratios in marine precipitation, Journal of Geophysical Research:
- 476 Atmospheres, 91, 6647–6658, https://doi.org/10.1029/jd091id06p06647, 1986.
- 477 Kesti, J., Asmi, E., O'Connor, E. J., Backman, J., Budhavant, K., Andersson, A., Dasari, S., Praveen,
- 478 P. S., Zahid, H., and Gustafsson, Ö.: Changes in aerosol size distributions over the Indian Ocean
- during different meteorological conditions, Tellus B Chem Phys Meteorol, 72,
- 480 https://doi.org/10.1080/16000889.2020.1792756, 2020.
- 481 Kirillova, E. N., Andersson, A., Sheesley, R. J., Kruså, M., Praveen, P. S., Budhavant, K., Safai, P.
- 482 D., Rao, P. S. P., and Gustafsson, Ö.: 13C- And 14C-based study of sources and atmospheric
- 483 processing of water-soluble organic carbon (WSOC) in South Asian aerosols, Journal of Geophysical
- 484 Research Atmospheres, 118, https://doi.org/10.1002/jgrd.50130, 2013.
- 485 Kirillova, E. N., Andersson, A., Tiwari, S., Srivastava, A. K., Bisht, D. S., and Gustafsson, Ö.: Water-
- 486 soluble organic carbon aerosols during a full New Delhi winter: Isotope-based source apportionment
- 487 and optical properties, J Geophys Res, 119, https://doi.org/10.1002/2013JD020041, 2014.
- 488 Krishnan, R., Sabin, T. P., Vellore, R., Mujumdar, M., Sanjay, J., Goswami, B. N., Hourdin, F.,
- Dufresne, J. L., and Terray, P.: Deciphering the desiccation trend of the South Asian monsoon
- 490 hydroclimate in a warming world, Clim Dyn, 47, 1007–1027, https://doi.org/10.1007/s00382-015-
- 491 2886-5, 2016.
- 492 Lana, A., Bell, T. G., Simó, R., Vallina, S. M., Ballabrera-Poy, J., Kettle, A. J., Dachs, J., Bopp, L.,
- 493 Saltzman, E. S., Stefels, J., Johnson, J. E., and Liss, P. S.: An updated climatology of surface
- 494 dimethylsulfide concentrations and emission fluxes in the global ocean, Global Biogeochem Cycles,
- 495 25, https://doi.org/10.1029/2010GB003850, 2011.
- 496 Lee, G., Ahn, J., Park, S. M., Moon, J., Park, R., Sim, M. S., Choi, H., Park, J., and Ahn, J. Y.: Sulfur
- 497 isotope-based source apportionment and control mechanisms of PM2.5 sulfate in Seoul, South Korea
- 498 during winter and early spring (2017–2020), Science of the Total Environment, 905,
- 499 https://doi.org/10.1016/j.scitotenv.2023.167112, 2023.
- 500 Lelieveld, J., Pozzer, A., Pöschl, U., Fnais, M., Haines, A., and Münzel, T.: Loss of life expectancy
- 501 from air pollution compared to other risk factors: A worldwide perspective, Cardiovasc Res, 116,
- 502 https://doi.org/10.1093/cvr/cvaa025, 2020.
- 503 Li, C., McLinden, C., Fioletov, V., Krotkov, N., Carn, S., Joiner, J., Streets, D., He, H., Ren, X., Li,
- 504 Z., and Dickerson, R. R.: India Is Overtaking China as the World's Largest Emitter of Anthropogenic
- 505 Sulfur Dioxide, Sci Rep, 7, https://doi.org/10.1038/s41598-017-14639-8, 2017.
- 506 Li, J., Carlson, B. E., Yung, Y. L., Lv, D., Hansen, J., Penner, J. E., Liao, H., Ramaswamy, V., Kahn,
- 507 R. A., Zhang, P., Dubovik, O., Ding, A., Lacis, A. A., Zhang, L., and Dong, Y.: Scattering and
- 508 absorbing aerosols in the climate system, https://doi.org/10.1038/s43017-022-00296-7, 1 June 2022.
- 509 McDuffie, E. E., Smith, S. J., O'Rourke, P., Tibrewal, K., Venkataraman, C., Marais, E. A., Zheng,
- 510 B., Crippa, M., Brauer, M., and Martin, R. V.: A global anthropogenic emission inventory of





- atmospheric pollutants from sector- And fuel-specific sources (1970-2017): An application of the
- 512 Community Emissions Data System (CEDS), Earth Syst Sci Data, 12, https://doi.org/10.5194/essd-
- 513 12-3413-2020, 2020.
- 514 Miyazaki, K.: TROPESS Chemical Reanalysis Aerosol SO4 6-Hourly 3-Dimensional Product V1,
- 515 https://doi.org/10.5067/TWDAYANXT8UM, 2024.
- Nair, H. R. C. R., Budhavant, K., Manoj, M. R., Andersson, A., Satheesh, S. K., Ramanathan, V., and
- 517 Gustafsson, Ö.: Aerosol demasking enhances climate warming over South Asia, NPJ Clim Atmos Sci,
- 518 6, https://doi.org/10.1038/s41612-023-00367-6, 2023.
- 519 Norman, A. L., Barrie, L. A., Toom-Sauntry, D., Sirois, A., Krouse, H. R., Li, S. M., and Sharma, S.:
- 520 Sources of aerosol sulphate at Alert: Apportionment using stable isotopes, Journal of Geophysical
- 521 Research Atmospheres, 104, https://doi.org/10.1029/1999JD900078, 1999.
- 522 Norman, A. L., Belzer, W., and Barrie, L.: Insights into the biogenic contribution to total sulphate in
- 523 aerosol and precipitation in the Fraser Valley afforded by isotopes of sulphur and oxygen, Journal of
- 524 Geophysical Research: Atmospheres, 109, https://doi.org/10.1029/2002jd003072, 2004.
- 525 Ram, K., Sarin, M. M., Sudheer, A. K., and Rengarajan, R.: Carbonaceous and secondary inorganic
- 526 aerosols during wintertime fog and haze over urban sites in the Indo-Gangetic plain, Aerosol Air Qual
- 527 Res, 12, https://doi.org/10.4209/aaqr.2011.07.0105, 2012.
- 528 Ramanathan, V., Crutzen, P. J., Lelieveld, J., Mitra, A. P., Althausen, D., Anderson, J., Andreae, M.
- 529 O., Cantrell, W., Cass, G. R., Chung, C. E., Clarke, A. D., Coakley, J. A., Collins, W. D., Conant, W.
- 530 C., Dulac, F., Heintzenberg, J., Heymsfield, A. J., Holben, B., Howell, S., Hudson, J., Jayaraman, A.,
- 531 Kiehl, J. T., Krishnamurti, T. N., Lubin, D., McFarquhar, G., Novakov, T., Ogren, J. A., Podgorny, I.
- 532 A., Prather, K., Priestley, K., Prospero, J. M., Quinn, P. K., Rajeev, K., Rasch, P., Rupert, S.,
- 533 Sadourny, R., Satheesh, S. K., Shaw, G. E., Sheridan, P., and Valero, F. P. J.: Indian Ocean
- 534 Experiment: An integrated analysis of the climate forcing and effects of the great Indo-Asian haze,
- Journal of Geophysical Research Atmospheres, 106, https://doi.org/10.1029/2001JD900133, 2001.
- 536 Ramarao, M. V. S., Ayantika, D. C., Krishnan, R., Sanjay, J., Sabin, T. P., Mujumdar, M., and Singh,
- 537 K. K.: Signatures of aerosol-induced decline in evapotranspiration over the Indo-Gangetic Plain
- 538 during the recent decades, Mausam, 74, 297–310, https://doi.org/10.54302/mausam.v74i2.6031, 2023.
- Randles, C. A., da Silva, A. M., Buchard, V., Colarco, P. R., Darmenov, A., Govindaraju, R.,
- 540 Smirnov, A., Holben, B., Ferrare, R., Hair, J., Shinozuka, Y., and Flynn, C. J.: The MERRA-2 aerosol
- reanalysis, 1980 onward. Part I: System description and data assimilation evaluation, J Clim, 30,
- 542 https://doi.org/10.1175/JCLI-D-16-0609.1, 2017.
- Rastogi, N., Agnihotri, R., Sawlani, R., Patel, A., Babu, S. S., and Satish, R.: Chemical and isotopic
- characteristics of PM10 over the Bay of Bengal: Effects of continental outflow on a marine
- 545 environment, Science of the Total Environment, 726, https://doi.org/10.1016/j.scitotenv.2020.138438,
- 546 2020.
- Rees, C. E., Jenkins, W. J., and Monster, J.: The sulphur isotopic composition of ocean water
- 548 sulphate, Geochim Cosmochim Acta, 42, https://doi.org/10.1016/0016-7037(78)90268-5, 1978.
- 549 Rodiouchkina, K.: Development of a multi-collector inductively coupled plasma mass spectrometry
- method for measurement of stable sulphur isotope ratios in aerosol sulphate (Dissertation), 2018.
- 551 Sawlani, R., Agnihotri, R., Sharma, C., Patra, P. K., Dimri, A. P., Ram, K., and Verma, R. L.: The
- 552 severe Delhi SMOG of 2016: A case of delayed crop residue burning, coincident firecracker
- $emissions, and a typical \ meteorology, Atmos \ Pollut \ Res, 10, \ https://doi.org/10.1016/j.apr.2018.12.015,$
- 554 2019.

https://doi.org/10.5194/egusphere-2025-5334 Preprint. Discussion started: 1 December 2025 © Author(s) 2025. CC BY 4.0 License.





- 555 Seguin, A. M., Norman, A. L., Eaton, S., Wadleigh, M., and Sharma, S.: Elevated biogenic sulphur
- dioxide concentrations over the North Atlantic, Atmos Environ, 44, 1139–1144,
- 557 https://doi.org/10.1016/j.atmosenv.2010.01.005, 2010.
- 558 Seguin, A. M., Norman, A. L., Eaton, S., and Wadleigh, M.: Seasonality in size segregated biogenic,
- anthropogenic and sea salt sulfate aerosols over the North Atlantic, Atmos Environ, 45,
- 560 https://doi.org/10.1016/j.atmosenv.2011.09.033, 2011.
- 561 Sharma, S. and Kumar, A.: Air pollutant emissions scenario for India Version 1, The Energy and
- Resources Institute, New Delhi, India, 2016.
- 563 Shenoy, D. M. and Kumar, M. D.: Variability in abundance and fluxes of dimethyl sulphide in the
- 564 Indian Ocean, in: Biogeochemistry, https://doi.org/10.1007/s10533-007-9092-4, 2007.
- 565 Szopa, S., V. Naik, B. Adhikary, P. Artaxo, T. Berntsen, W.D. Collins, S. Fuzzi, L. Gallardo, A.
- 566 Kiendler-Scharr, Z. Klimont, H. Liao, N. Unger, and P. Zanis, 2021: Short-Lived Climate Forcers. In:
- 567 Climate Change 2021: The Physical Science Basis. Contribution of Working Group I to the Sixth
- Assessment Report of the Intergovernmental Panel on Climate Change [Masson-Delmotte, V., P.
- 569 Zhai, A. Pirani, S.L. Connors, C. Péan, S. Berger, N. Caud, Y. Chen, L. Goldfarb, M.I. Gomis, M.
- 570 Huang, K. Leitzell, E. Lonnoy, J.B.R. Matthews, T.K. Maycock, T. Waterfield, O. Yelekçi, R. Yu,
- and B. Zhou (eds.)]. Cambridge University Press, Cambridge, United Kingdom and New York, NY,
- 572 USA, pp. 817–922, doi: 10.1017/9781009157896.008.
- Verma, S., Boucher, O., Shekar Reddy, M., Upadhyaya, H. C., Le Van, P., Binkowski, F. S., and
- 574 Sharma, O. P.: Tropospheric distribution of sulphate aerosols mass and number concentration during
- 575 INDOEX-IFP and its transport over the Indian Ocean: A GCM study, Atmos Chem Phys, 12,
- 576 https://doi.org/10.5194/acp-12-6185-2012, 2012.
- 577 Wadleigh, M. A.: Sulphur isotopic composition of aerosols over the western North Atlantic Ocean, in:
- 578 Canadian Journal of Fisheries and Aquatic Sciences, https://doi.org/10.1139/F04-073, 2004.
- 579 Winiger, P., Andersson, A., Yttri, K. E., Tunved, P., and Gustafsson, Ö.: Isotope-Based Source
- 580 Apportionment of EC Aerosol Particles during Winter High-Pollution Events at the Zeppelin
- 581 Observatory, Svalbard, Environ Sci Technol, 49, https://doi.org/10.1021/acs.est.5b02644, 2015.
- 582 World Health Organization: WHO global air quality guidelines: particulate matter (PM2.5 and
- PM10), ozone, nitrogen dioxide, sulfur dioxide and carbon monoxide, 2021.

584

585